Journal of Sustainable Development of Smart Energy Networks

https://www.sdewes.org/jsdsen

Year 2026, Volume 1, Issue 4, 2030728

*Original Research Article*

# Overcoming Constraints for Fair Energy: Compatible Solutions in Heritage Protected Urban Centres

***Andrea Palmieri[*1], Paolo Maria Congedo[1], Cristina Baglivo[1], Pio Alessandro Lombardi[2], Przemyslaw Komarnicki[3]***

[1]Department of Engineering for Innovation, University of Salento, Lecce, Italy
e-mail: andrea.palmieri@unisalento.it, paolo.congedo@unisalento.it, cristina.baglivo@unisalento.it

[2] Fraunhofer Institute for Factory Operation and Automation IFF, Magdeburg, Germany
e-mail: pio.lombardi@iff.fraunhofer.de

[3] Magdeburg-Stendal University of Applied Sciences, Magdeburg, Germany
e-mail: przemyslaw.komarnicki@h2.de

Cite as: Palmieri, A., Congedo, P. M., Baglivo, C., Lombardi, P. A., Komarnicki, P., Overcoming Constraints for Fair Energy: Compatible Solutions in Heritage Protected Urban Centres, J. sustain. dev. smart. en. net., 1(4), 2030728, 2026, DOI: https://doi.org/10.13044/j.sdsen.d3.0728



## ABSTRACT

Decarbonizing historic urban centres is challenging due to strict architectural and landscape conservation constraints, which limit conventional energy efficiency and renewable solutions. This study investigates three districts in the UNESCO-protected historic centre of Quedlinburg (Germany), assessing the potential of integrated interventions including internal wall insulation, window upgrades, hybrid heating systems, and building-integrated photovoltaics (BIPV). Results indicate that envelope improvements combined with hybrid gas boiler–air/water heat pump systems reduce heating demand by over 35%, with a further 10% decrease under projected 2050 climate conditions. BIPV integration contributes to an approximately 30–35% reduction in non-renewable primary energy, depending on roof orientation and available surface area. hDistrict-level analysis confirms the scalability of these measures, demonstrating that conservation-compatible strategies can achieve significant energy and emissions reductions while respecting heritage constraints, providing a replicable framework for other historic centres.

## KEYWORDS

*Climate change, Energy transition, Historic buildings, Energy consumption, Decarbonization, Energy efficiency, Building-integrated photovoltaics, Heat pumps.*

## INTRODUCTION

The climate emergency represents a critical challenge for several sectors of contemporary society, particularly the construction sector, which accounts for a significant share of global energy consumption and greenhouse gas emissions [1,2]. In response to this challenge, numerous climate mitigation policies have been implemented worldwide, involving substantial economic and social transformations aimed at reducing carbon emissions [3].

At the European level, the energy transition is being driven by strategic initiatives such as the Green Deal and the "Fit for 55" package, which aim to address climate change while

[*] Corresponding author

promoting sustainability and social equity [4]. Within this framework, the renovation of historic buildings plays a crucial role, as it seeks to improve their energy performance while enabling the integration of renewable energy sources.

Citizens play an active role in this transformation and, through local cooperation, can establish Renewable Energy Communities (RECs), local entities in which energy produced from renewable sources is shared among members. RECs represent an innovative model that enables not only the collective production of clean energy but also the participatory management of energy resources, fostering an energy transition that is technically feasible, fair, and sustainable while generating widespread benefits for the entire community.

The direct involvement of citizens promotes greater awareness and empowerment, which are essential elements for overcoming technical and economic barriers in these contexts [5,6,7]. Energy sharing within RECs also contributes to a more efficient management of loads on the electricity grid, reducing consumption peaks that may place stress on infrastructure by balancing energy supply and demand.

However, there are many obstacles along the way. In urban contexts subject to historical and artistic protection or recognized as UNESCO heritage sites, architectural, conservation and cultural regulatory constraints make it difficult to install sustainable technologies, such as photovoltaic (PV) panels, or to adopt efficiency measures [8,9].

Recent research has highlighted the potential of digital platforms based on digital twin technology to support decision-making in UNESCO protected historic centres [10]. The growing complexity of sustainable urban planning in European cities calls for innovative digital tools capable of integrating multiple disciplines (energy, economy, and spatial development) within a unified framework [11].

This context gives rise to a general reflection on the presumed balance between technological innovation and heritage conservation. While the need to reduce emissions through the use of renewable sources is immediate, there is a widespread perception of incompatibility between PV systems and the historical and architectural context in which they are to be installed.

These urban environments are characterized by historic buildings that offer urban spaces for both residents and tourists. Consequently, it is important to preserve the visual appearance by using materials and construction techniques that are well integrated with the original architectural structures [12].

Historic buildings are often constructed from materials that require specific heating requirements, which are 8-10 times higher than those of low-energy buildings, resulting in higher energy bills [13]. Urgent action is therefore needed in certain urban contexts characterized by the presence of historic buildings. Energy efficiency improvements require the use of insulating materials [14], but the historic value of the buildings often prevents the external application of such materials. The only possible solution is therefore internal insulation, which is one of the most complicated energy efficiency measures to implement [15].

In addition to the opaque envelope, another important area of intervention is that of transparent surfaces, i.e. windows, which represent one of the greatest points of energy loss. The ideal solution would be to replace them completely with other windows with high energy performance, but even in this case, in restricted urban centres, this is inappropriate, as the original openings play an architectural and identity-defining role. Historic windows are often made of high-quality wood, so restoration of surface deterioration together with improvements such as replacing seals, adding internal storm windows or installing double glazing offer a good margin for improving the thermal performance of windows [16,17].

Achieving sustainable urban management is a necessary step in resisting the impacts of climate change. The lack of adequate and efficient energy services not only limits the possibility of reducing carbon emissions but is also a critical issue that directly contributes to the vulnerabilities associated with energy poverty [18,19]. In these contexts, regulations impose restrictions to protect historic buildings or cultural heritage from interventions that undermine authenticity [20], thus creating a form of energy inequality that goes beyond economic issues alone. Residents in these contexts, regardless of income, have fewer tools at their disposal to reduce consumption, lower utility bills and promote indoor comfort. In these protected urban centres, it can be said that energy poverty is not always linked solely to the economic vulnerability of residents but is compounded by an additional regulatory vulnerability that restricts opportunities for self-production and access to renewable sources [21].

Recent studies highlight the role of ventilation strategies in ensuring indoor thermal comfort while reducing energy requirements, particularly in Mediterranean climates. Simulations demonstrate that, when combined with an efficient building envelope, modulating air exchange rates can maintain acceptable thermo-hygrometric comfort conditions and significantly reduce or eliminate the need for conventional heating systems. These approaches contribute to improving indoor environmental quality and climate resilience, particularly in public and school buildings [22, 23].

However, recent developments in the field of architectural integration show that it is possible to combine clean energy production with respect for the historical identity of places. Compatibility of high-end aesthetic solar modules, systems installed in building materials and design guidelines geared towards them are real tools through which to overcome the apparent hostility between conservation and innovation. A more flexible and interdisciplinary vision can thus provide new horizons, transforming limitations into opportunities to build low-impact solutions with high symbolic value. The goal is not to compromise historical memory, but to make it an active part of change [24]. In this direction, certain solution technologies are gaining popularity, such as building-integrated photovoltaic (BIPV) panels, thanks to their aesthetic resistance to constrained architectural contexts. A clear example is provided by coloured PV modules, designed to blend in visually with traditional materials and limit their impact on the landscape. However, these technologies have a significant drawback: the colouring and aesthetic treatments applied to the surface cause partial shading of the cells, resulting in reduced efficiency and electricity production [25].

This study focuses on technical and design analysis in the city of Quedlinburg (Saxony-Anhalt, Germany), recognized as a UNESCO World Heritage Site in 1994, where landscape and architectural restrictions make the adoption of sustainable technologies challenging. The aim is to explore the potential for electricity generation using BIPV panels and to reduce heating demand through interventions compatible with conservation regulations, such as internal insulation and window replacement. Furthermore, the integration of hybrid technologies, consisting of gas boilers and air-to-water heat pumps, into traditional heating systems is being evaluated [26,27,28]. The data used are derived from on-site surveys of a real building and used in energy simulations performed with Termolog Epix 15, considering two climate scenarios for the years 2006 and 2050.

The results indicate that, despite stringent constraints, it is possible to initiate urban decarbonization processes in certain urban contexts through the implementation of compatible technical solutions, with economic and environmental benefits.

Despite the extensive literature on the energy renovation of historic and protected buildings, many studies focus on individual technologies or assessments limited to current climatic conditions, often neglecting integrated analyses and the medium- to long-term impacts of climate change.

Few studies jointly address conservation compatible envelope measures, hybrid heating systems, and BIPV integration under future climate scenarios, particularly at district scale in UNESCO-protected urban contexts, where regulatory and morphological constraints further decarbonization strategies.

To address this gap, this study develops and applies an integrated multi-technology, multi-scenario assessment framework, combining conservation-compatible building envelope interventions, hybrid thermal generation systems and BIPV integration. The framework is evaluated under both current and projected future climate conditions and extended from the building scale to the district scale in the UNESCO-protected city of Quedlinburg, with the aim of assessing the energy performance of the proposed solutions and their transferability to other historic centres subject to similar constraints.

Specifically, the study aims to address the following research objectives:

1. Assess the extent to which conservation-compatible redevelopment measures can reduce heating energy requirements in a historic center subject to protection constraints.
2. Analyze the influence of future climatic conditions on the energy performance of renovated buildings in the medium to long term.
3. Quantify the contribution of integrated photovoltaic systems (BIPV) to the reduction of non-renewable primary energy at district level, as a possible lever for energy transition in protected areas.

## METHODOLOGY

## CASE STUDY DESCRIPTION

### Regulatory context

Quedlinburg is a medieval town in the state of Saxony-Anhalt, Germany, which has been listed as a UNESCO World Heritage Site since 1994. The historic centre of the town is characterized by an urban structure consisting of courtyards with half-timbered buildings.

The high cultural and architectural value of the buildings has led to the adoption of strict conservation restrictions. In addition to complying with UNESCO guidelines, the town is subject to the *Denkmalschutzgesetz* of the state of Saxony-Anhalt, the regional law on the protection of historical monuments, which strictly regulates the methods of intervention on protected buildings and areas [29]. This legislation represents a significant barrier to the adoption of innovative energy solutions in historic areas, requiring technical approaches that balance protection and sustainability. The historic centre of Quedlinburg, with its wealth of listed buildings, is thus a prime example of the tension between conservation and innovation.

The integration of renewable technologies and energy efficiency measures is limited by strict landscape constraints and the need to preserve the historical integrity of the buildings. Despite these constraints, many buildings have high energy consumption and inefficiencies due to the shortcomings of traditional structures.

The challenges in this context are not only technical but also require an integrated approach that considers energy needs, regulatory constraints and cultural sensitivities.

### Climate data

Quedlinburg is located in an area with a cool temperate climate, classified as climate zone 2 according to German standard DIN 4108-2:2013-02 [30]. This classification implies a reference indoor temperature of 20 °C and a winter design external temperature of -12 °C. The average number of degree days (DD) is approximately 3400, indicating the need for adequate building design to ensure indoor thermal comfort throughout the year, especially in the coldest winter months. According to international classifications, such as Köppen-Geiger, Quedlinburg is classified as Cfb, typical of temperate oceanic climates [31]. This type of climate is characterized by cool summers, relatively harsh winters and evenly distributed rainfall throughout the year.

Figure 1 shows the variation in external temperature in Quedlinburg, comparing climate data for 2006 and 2050. In the two climate scenarios, the average temperature varies from

9.87 °C to 11.25 °C, the minimum temperature from -14.55 °C to -11.20 °C, while the maximum temperature remains virtually unchanged.

The climate data for 2006 was obtained from the Renewables.ninja [32] website, based on official meteorological archives, and consists of complete hourly data (8,760 hours) representative of the actual climatic conditions in the Quedlinburg area during the period analysed.

For the future scenario 2050, the hourly climate dataset generated with Meteonorm software was used, based on the IPCC RCP 4.5 scenario [33].

The use of observational data for the historical scenario and modelled data for the future scenario reflects the different nature of the two analyses: retrospective and prospective.

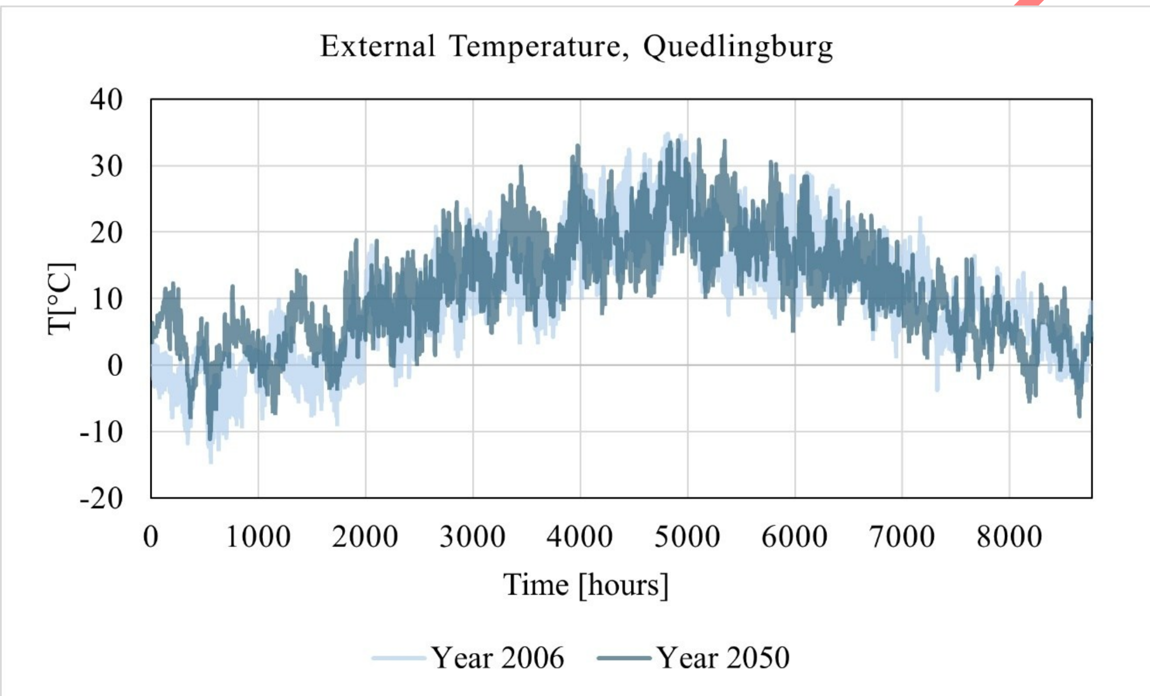


Figure 1 External temperature Quedlinburg

## DISTRICTS ANALYSED

The work is based on a real prototype model of the city of Quedlinburg, developed to faithfully represent the typical building characteristics of the historic centre. This model was subsequently used to analyse three districts, identified as District 1, District 16 and District 17, characterized by comparable building typologies, construction materials and geometric features, including roof pitch, as shown in Figure 2. **the potential interaction between renewable generation and the building's demand.** Each district was delimited on the basis of the road network surrounding it, taking as boundaries the streets that clearly define its spatial extent:

- District 1 is bordered by Breite Straße, Hölle, Markt, Pölle, Schuhhof and Stieg.
- District 16 is bordered by Blasiistraße, Carl-Ritter Straße, Hohe Straße, Markt, Word, and Wordgasse.
- District 17 is bordered by Blasiistraße, Hohe Straße and Markt.

Figure 2 shows a bird's-eye view of the three districts of the historic centre under study. For easy identification, the districts have been highlighted in three different colours: purple for District 1, red for District 16 and green for District 17.

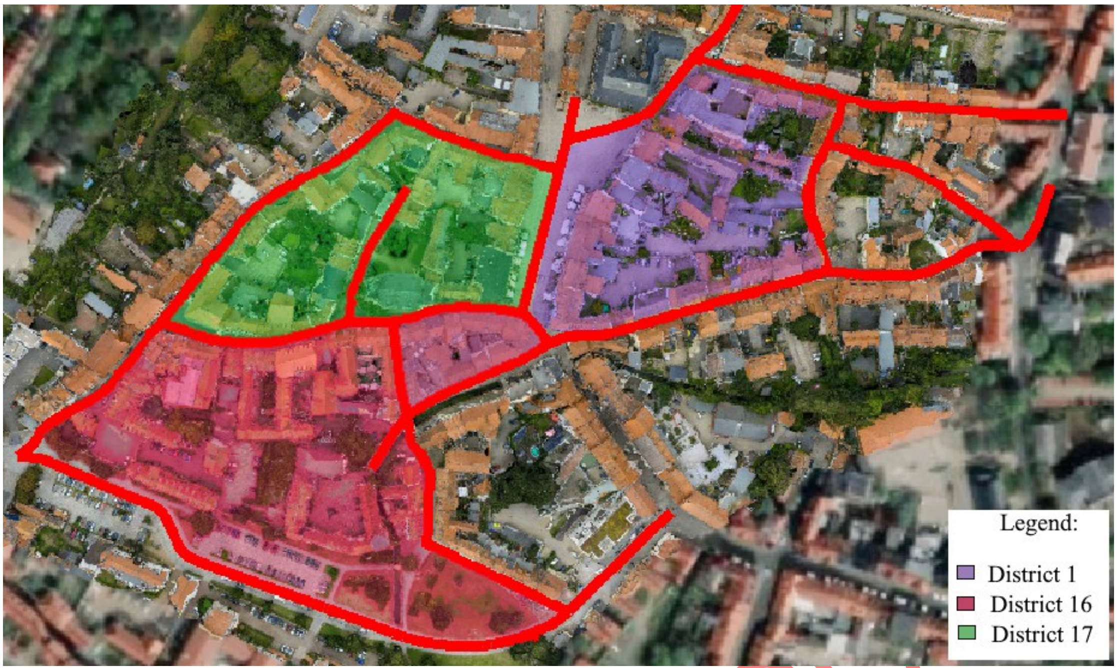


Figure 2 View from above of the three districts under study: District 1, District 16, District 17

## PROTOTYPE MODEL

The energy analysis of the prototype model is based on the modelling of Haus Grünhage, a historic building in the old town of Quedlinburg that is representative of the city’s traditional building types. The geometric floor plan of the first floor and the main façade of this building were known, as well as construction information regarding the load-bearing wall structure, built using the wooden truss technique typical of the region. The building has four floors above ground with a floor area of 234.99 $m^2$, reaching a total height of 20.24 m. The top floor consists of a pitched roof with a slope of 40°, whose ridge line is 6.73 m above the floor level. The roof is made of typical reddish tiles, which are a recurring feature in the residential architecture of the city's historic districts. Figure 3 shows the geometric plan of the building, the main elevation and a photograph of the actual elevation.

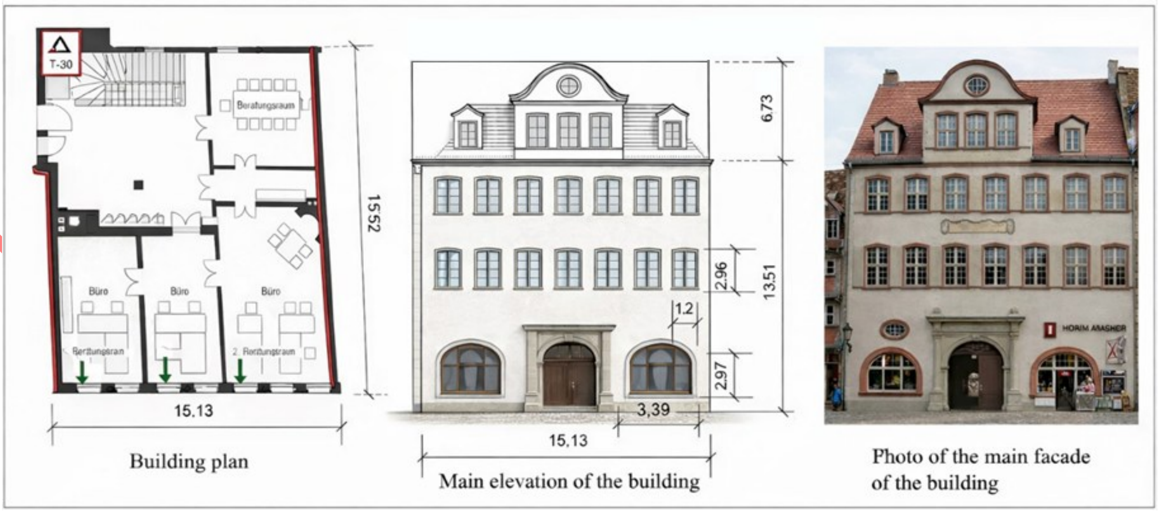


Figure 3 Geometric plan, main elevation and photograph of the façade of the real building.

The building’s energy model was developed in TERMOLOG Epix 15 [34] using hourly simulation, in order to assess the energy performance indices for winter heating, domestic hot water production and overall energy performance. In the case analysed, the occupancy profile assumed is residential and is automatically assigned by the software based on the building's intended use. In line with this approach, internal heat gains are also generated automatically according to a weekly hourly profile that distinguishes between weekdays and weekends. Specifically, from Monday to Friday, internal loads amount to 756 W during the 00:00–06:00 and 23:00–24:00 periods, 378 W in the 07:00–09:00 and 17:00–19:00 time slots, 76 W in the 10:00–13:00 time slot, 151 W in the 14:00–16:00 time slot and 605 W in the 20:00–22:00 time slot. For Saturdays and Sundays, the profile maintains a value of 756 W during the periods 00:00–06:00 and 23:00–24:00, whilst during the remaining hours of the day the internal load is 605 W.

For the post-intervention configuration, the heating system was modelled as a hybrid system comprising a gas boiler and an air-to-water heat pump, integrated with an existing system fitted with radiators. The heat pump has a nominal heat output of 11.20 kW and a COP of 3.85, with the flow temperature set at 55 °C. The model also considers a deterioration coefficient at partial loads of 0.90, in accordance with the UNI EN 14825 standard, and a minimum outdoor operating temperature of -15 °C. The system control logic was represented using on/off mode and a parallel bivalence scheme: the heat pump operates with priority to meet the heating demand, whilst the boiler intervenes to supplement it during periods of high load or when the power output from the heat pump is insufficient to fully meet the building's demand. The same system configuration was maintained in both climate scenarios analysed, in order to isolate the effect of climatic variations on energy performance without introducing further variables linked to technological changes in the generation system.

The analysis also took into account potential long-term technological improvements in PV modules. According to recent projections on the evolution of PV technologies, the average efficiency of silicon modules is expected to rise from around 22.6% in 2022 to around 28.7% in 2050, mainly due to the widespread adoption of high-efficiency cell architectures such as TOPCon, SHJ and IBC [36]. Based on these projections, an efficiency improvement coefficient of 1.27 was therefore defined, obtained from the ratio between the average efficiency forecast for 2050 and that observed in 2022. This coefficient was applied proportionally to the efficiency of the BIPV modules used in the study in order to represent the expected technological improvement in the 2050 scenario, whilst keeping the architectural characteristics of the system and the installable surface area unchanged.

Hourly climate files for Quedlinburg (years 2006 and 2050) were imported into the software; 2006, characterized by a particularly harsh winter, was used as a conservative scenario, while 2050 represents a future scenario to assess the impacts of climate change. Figure 4 shows the 3D energy model of the analysed building.

Figure 4 Three-dimensional energy model of the analysed building (Haus Grünhage).

The definition of a valid energy model for Haus Grünhage made it possible to obtain results that could be extended to the entire sample of buildings comprising the three historic districts of the city of Quedlinburg. The extension was carried out by assuming the repeatability of the energy characteristics of the reference building across the entire building fabric of the districts.

The extension of the results from the single prototype building to the district scale is based on the proven typological, morphological, and constructional homogeneity that characterizes the historic centre of Quedlinburg, recognized as a UNESCO site. The urban fabric is mainly composed of buildings belonging to the same construction period, with similar geometric configurations, similar wall stratigraphy, and comparable traditional plant solutions.

The building selected for analysis was considered representative of the prevailing building typology, in terms of both size and the thermophysical characteristics of the envelope and heating system configuration. This choice is not an arbitrary generalization but derives from the architectural and constructional consistency that defines the urban context under study.

Although the extension of the building prototype to the district level is supported by the marked typological, morphological and structural homogeneity of the urban fabric analysed, this extrapolation should be interpreted as a comparative extrapolation based on typology rather than as a building-by-building prediction. Individual buildings may in fact differ in terms of condition, level of maintenance, actual use, occupancy patterns, system operation and previous refurbishment works; these sources of variability have not been modelled separately.

For this reason, the proposed approach is better suited to identifying relative trends, comparative energy benefits and decarbonisation potential at the district level rather than accurately predicting the performance of each individual building. However, the degree of homogeneity within the historic building stock makes the selected prototype a methodologically valid benchmark for assessing the overall impact of the interventions analysed at the district level.

Furthermore, in order to assess the contribution of renewable energy sources provided by integrated PV panels, the buildings in the three districts were classified according to the available roof area, divided into five size ranges (0–20 m², 20–50 m², 50–100 m², 100-150 m² and over 150 m²). Within each group, the prevailing exposure of the roofs (south, east and west) was also considered in order to take into account the different solar radiation conditions and obtain a more realistic estimate of the PV production potential. The roof areas of the individual building units were surveyed using the Dronodat 3D Viewer online platform [37], which allows interactive analysis and measurement of roofs using three-dimensional models of the city of Quedlinburg. An example of the three-dimensional representation of the urban area used for the analysis is shown in Figure 5. The analysis considered only roof areas that were actually suitable for the installation of PV modules, excluding areas occupied by chimneys, skylights or other architectural elements that could have reduced the usable area. This classification made it possible to estimate the photovoltaic production potential more accurately by considering both the size of the available areas and their orientation.

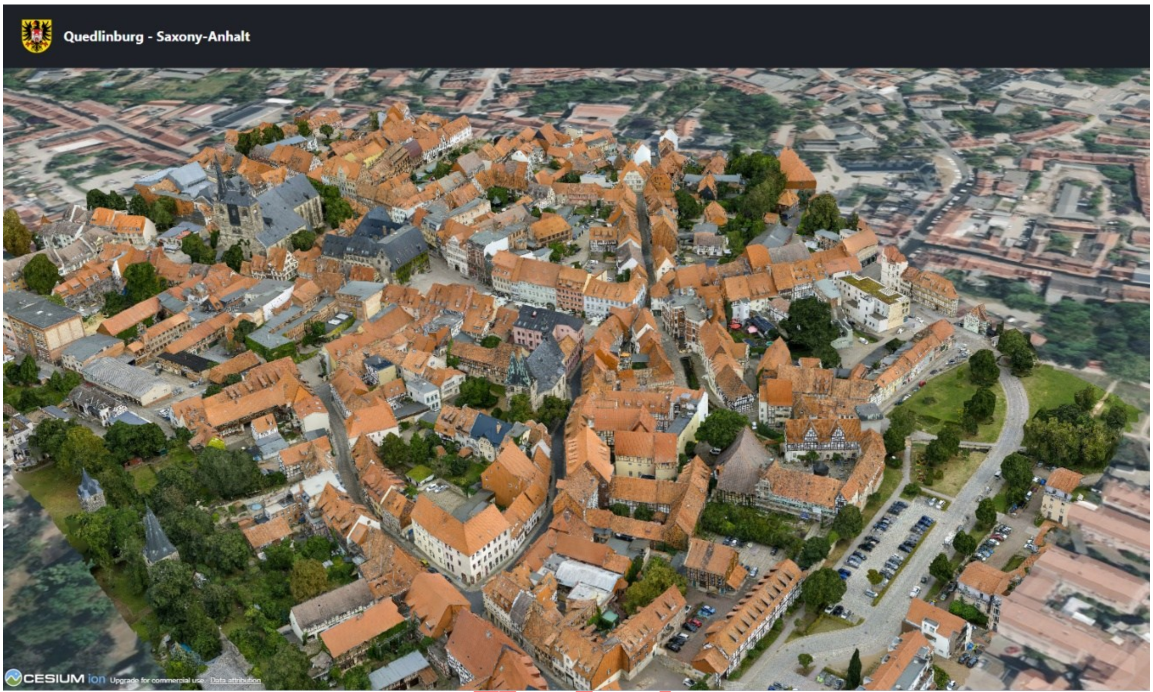


Figure 5 Three-dimensional view of the city of Quedlinburg used for the analysis of roof surfaces.



*Table 1* below summarises the number of roofs falling within the different ranges depending on the orientation of the three districts analysed.

Table 1. Distribution of the number of buildings by roof surface area interval and roof orientation, divided by district.

| Interval Roof Surface [$m^2$] | Number of buildings by orientation | | | District |
|---|---|---|---|---|
| | South | East | West | |
| 0-20 | 5 | - | 3 | |
| 20-50 | 18 | 1 | 4 | |
| 50-100 | 10 | - | 4 | 1 |
| 100-150 | 5 | - | 2 | |
| >150 | 1 | - | 2 | |
| 0-20 | 9 | 4 | 8 | |
| 20-50 | 16 | - | 11 | |
| 50-100 | 11 | - | 14 | 16 |
| 100-150 | 3 | - | - | |
| >150 | 1 | - | - | |
| 0-20 | 2 | - | 3 | 17 |

| | | | |
|---|---|---|---|
| 20-50 | 11 | 2 | 12 |
| 50-100 | 6 | 0 | 8 |
| 100-150 | 2 | - | 3 |
| >150 | 2 | - | - |

The analysis and modelling of energy requirements were carried out considering various intervention scenarios that simulate the application of efficiency technologies compatible with the protection constraints imposed on UNESCO heritage sites. In the initial phase, the energy simulations reproduced the current state of the buildings without significant redevelopment, considering the climatic conditions of 2006, taken as a reference year representative of current climatic conditions, and a future climate scenario for 2050, used to assess the effects of climate change on the energy performance of buildings. In subsequent scenarios, improvements were made to the building envelope and systems, such as the application of a layer of internal insulation to the walls, the replacement of single-glazed windows with low-transmittance double-glazed windows, the installation of integrated PV systems on sloping roofs and, finally, the integration of traditional gas boilers with electric heat pumps for the combined production of heating and domestic hot water.

The systematic comparison of the results obtained in the different scenarios made it possible to quantify the energy benefits deriving from individual interventions and their combinations, while highlighting the technical and spatial limitations that characterise the historical context under consideration.

**Characteristics of the structural elements**

In the energy modelling, the stratigraphy of the building envelope elements was defined (Figures 6-7).

The external half-timbered wall, typical of local construction, consists of a mixed wood-solid brick structure, with a distribution of 33% wooden elements and 66% solid bricks. In order to improve its energy performance, an internal insulation layer of calcium hydrate silicate was added. The resulting thermal transmittance is U = 0.430 W/m²K.

The intermediate floor is characterised by a wooden structure with traditional filling and has an equivalent transmittance of U = 0.451 W/m²K. The ground floor, built on a wooden structure separated from the ground, has a value of U = 1.167 W/m²K.

The pitched roof, representative of the local architectural style, was modelled to include a layer of rock wool insulation, achieving a transmittance of U = 0.474 W/m²K.

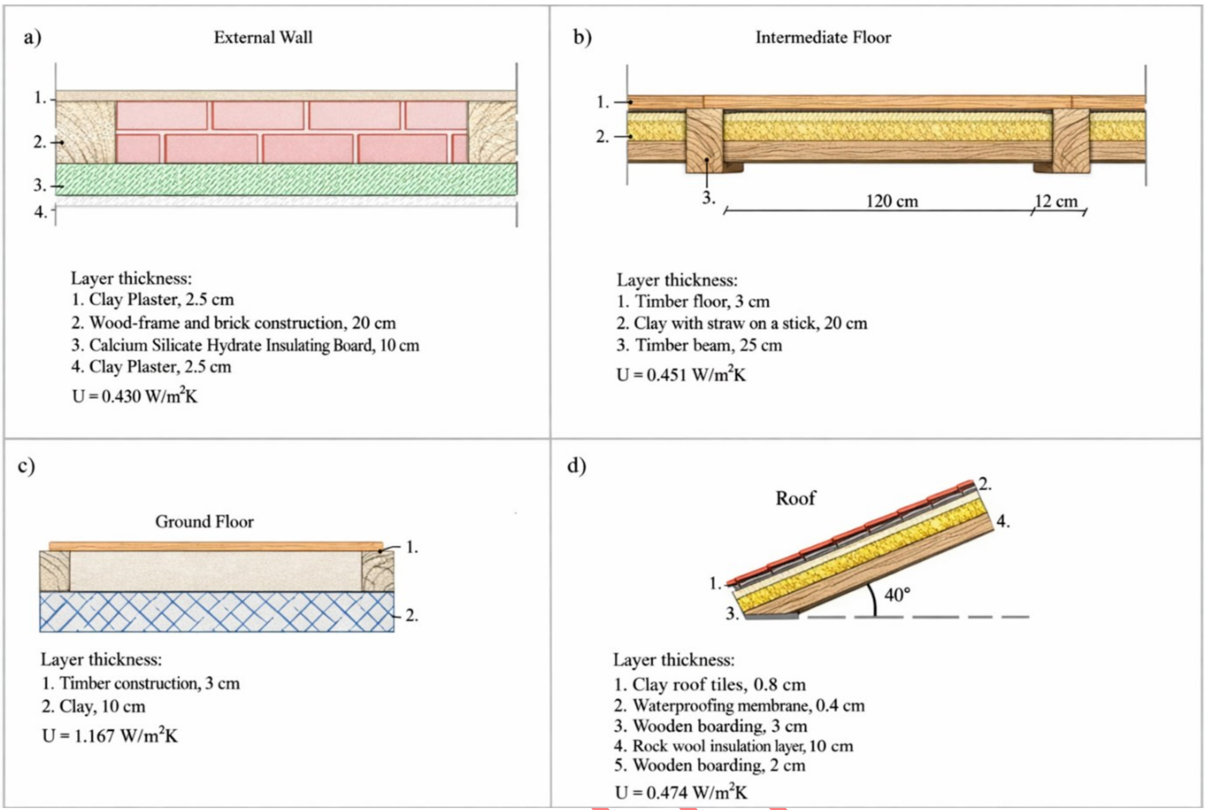


Figure 6. Construction layers of the building envelope structures.

In the energy modelling of the building, the original wooden fixtures were taken into account, both for the windows and the entrance door. For the windows, the analysis was first conducted assuming the presence of single glazing and then evaluating the adoption of double glazing of type 4.16.4 (Argon), in order to highlight the improvement in performance.

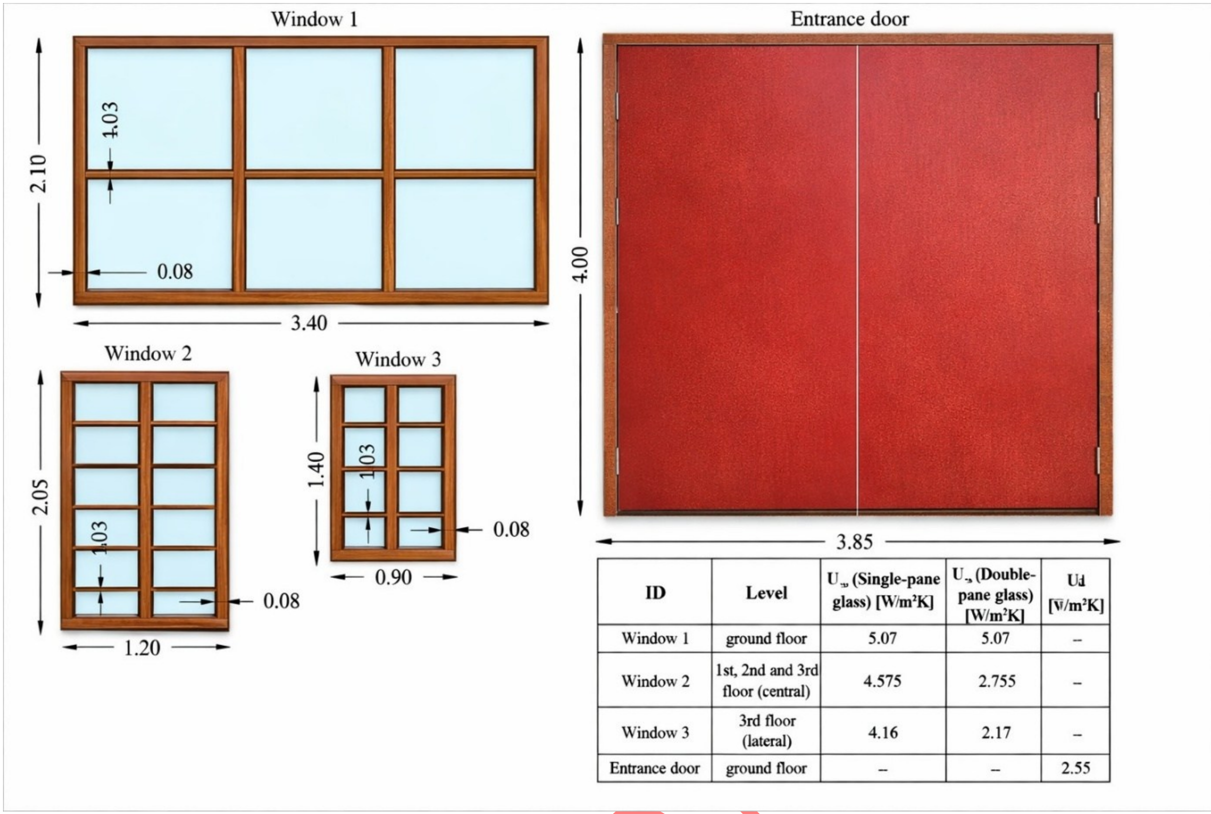


| ID | Level | $U_w$ (Single-pane glass) $[W/m^2K]$ | $U_w$ (Double-pane glass) $[W/m^2K]$ | $U_d$ $[W/m^2K]$ |
|---|---|---|---|---|
| Window 1 | ground floor | 5.07 | 5.07 | – |
| Window 2 | 1st, 2nd and 3rd floor (central) | 4.575 | 2.755 | – |
| Window 3 | 3rd floor (lateral) | 4.16 | 2.17 | – |
| Entrance door | ground floor | – | – | 2.55 |

Figure 7. Geometric and thermal characteristics of doors and windows



## Results and discussions

This section presents the results obtained from the energy simulation of the building model analysed, chosen as representative of the traditional construction types in the city of Quedlinburg.

Two main configurations were considered during the analysis:

- a pre-intervention (reference) scenario, representative of the building in its original state, characterised by a poorly performing envelope and a heating system based on a traditional boiler;
- a post-intervention (renovated) scenario, which includes the improvement of the building envelope through internal insulation of opaque surfaces and replacement of windows with double glazing, as well as the adoption of a hybrid system consisting of a boiler and an air-to-water heat pump (ASHP).

The sample building was initially analysed as a reference case for estimating energy requirements for space heating and domestic hot water (DHW) production. The results obtained for the prototype model were then extended to three selected districts in order to assess the impact of redevelopment strategies and climatic conditions at the district scale.

### Reference building: comparison between pre- and post-intervention scenarios

The comparison between the two climate scenarios (*Tables 2 and 3*) shows a systematic reduction in heating requirements in 2050 compared to 2006, with an average decrease of about 10%, attributable to the increase in winter temperatures. This variation, already observable in the original configuration of the building (*Table 2*), confirms the influence of climate change on seasonal energy performance.

However, the impact of the renovation strategy is significantly more pronounced (*Table 3*). The combination of internal insulation of the building envelope, replacement of windows and doors, and adoption of a hybrid boiler-heat pump system allows for a reduction in heating requirements of more than one-third compared to the initial configuration, under the same climatic conditions. This result demonstrates that the main factor in energy improvement is not climate change, but rather the adoption of technological solutions compatible with conservation constraints.

With regard to domestic hot water production, the results (*Tables 2 and 3*) show a reduction in 2050 compared to 2006, mainly due to the decrease in the temperature difference between mains water and usage temperature. The useful demand for DHW remains substantially independent of the system configuration, as it is determined mainly by climatic conditions and consumption profiles rather than by the generation system adopted.

Overall, the analysis of the reference model shows that the impact of energy-efficiency refurbishment measures is significantly greater than that caused by climate change. The reduction in heating demand achieved through improvements to the building envelope and the adoption of a hybrid system is, in fact, approximately three times greater than the reduction attributable solely to climatic variations between the 2006 and 2050 scenarios. This result highlights how retrofit strategies represent the main factor in reducing energy consumption, even in changing climatic contexts.

Table 2. Thermal energy demand ($EP_{H,nd}$ and $EP_{W,nd}$) of the prototype building in the original configuration, under the 2006 and 2050 climate scenarios.

| Original envelope and boiler system | | | | |
|---|---|---|---|---|
| THERMAL ENERGY REQUIREMENTS | YEAR 2006 | | YEAR 2050 | |
| $EP_{H,nd}$ | 93.29 | kWh/m² | 84.39 | kWh/m² |
| $EP_{W,nd}$ | 7.57 | kWh/m² | 2.91 | kWh/m² |

Table 3. Thermal energy demand ($EP_{H,nd}$ and $EP_{W,nd}$) of the prototype building after renovation, under the 2006 and 2050 climate scenarios.

| Improved building envelope and hybrid boiler + air-water heat pump system | | | | |
|---|---|---|---|---|
| THERMAL ENERGY REQUIREMENTS | YEAR 2006 | | YEAR 2050 | |
| $EP_{H,nd}$ | 60.68 | kWh/m² | 54.65 | kWh/m² |
| $EP_{W,nd}$ | 7.57 | kWh/m² | 2.91 | kWh/m² |

**Integration of photovoltaic systems**

The integration of Building-Integrated Photovoltaic (BIPV) systems was analysed to evaluate their contribution to reducing non-renewable primary energy in the reference building (*Table 4*). A more detailed reading of the results shows that the effect of BIPV integration is non-linear and depends heavily on roof orientation and available surface area.

For south-facing roofs, the $EP_{gl,nren}$ decreases from 48.63 to 34.85 kWh/m² in 2006 and from 40.24 to 26.41 kWh/m² in 2050 when moving from the 0–20 m² class to the 100–150 m² class, corresponding to reductions of approximately 28% and 34%, respectively. West-facing roofs show a similar trend, although with slightly lower annual performance in the smaller classes; they remain effective in the larger classes, with $EP_{gl,nren}$ decreasing from 49.50 to 36.10 kWh/m² in 2006 and from 42.02 to 27.14 kWh/m² in 2050 between the 0–20 m² and >150 m² classes. East-facing roofs show more moderate reductions across the available classes, confirming the influence of orientation on annual solar yield.

The results also highlight a saturation effect. Specifically, for south-facing roofs, the transition from the 100–150 m² class to the >150 m² class produces only a negligible additional reduction in $EP_{gl,nren}$. This indicates that, beyond a certain installed area, photovoltaic generation increasingly exceeds the building's demand, and the excess electricity is primarily exported to the grid. Consequently, further increases in the installed surface area do not yield proportional improvements in the building-scale energy performance index.

Furthermore, the comparison between the 2006 and 2050 scenarios shows that the same BIPV configuration leads to lower $EP_{gl,nren}$ values in the future climate scenario for all available orientations. This result reflects the combined effect of reduced heating demand under milder climatic conditions and the assumed improvement in photovoltaic module efficiency. Overall, Table 4 demonstrates that the energy benefit of BIPV systems depends not only on the installed area but also on the interaction between roof orientation, building demand, and the saturation of on-site energy use, with south-facing roofs and medium-to-large surface areas representing the most effective configuration in the case analysed.

Table 4. Global energy demand performance indices ($EP_{gl,nren}$, $EP_{gl,ren}$, $EP_{gl,tot}$) of the prototype building under different roof orientations and photovoltaic surface intervals, for the 2006 and 2050 climate scenarios.

| | | | Year 2006 | | | Year 2050 | | |
|---|---|---|---|---|---|---|---|---|
| Orientation | Surface interval | PV system case | $EP_{gl,nren}$ [kWh/m²] | $EP_{gl,ren}$ [kWh/m²] | $EP_{gl,tot}$ [kWh/m²] | $EP_{gl,nren}$ [kWh/m²] | $EP_{gl,ren}$ [kWh/m²] | $EP_{gl,tot}$ [kWh/m²] |
| South | 0-20 | 0-20 | 48.63 | 40.96 | 89.6 | 40.24 | 33.58 | 73.82 |
| | 20-50 | 20-50 | 45.2 | 41.9 | 87.09 | 36.2 | 34.68 | 70.88 |
| | 50-100 | 50-100 | 40 | 43.31 | 83.31 | 30.41 | 36.25 | 66.66 |
| | 100-150 | 100-150 | 34.85 | 44.71 | 79.56 | 26.41 | 37.34 | 63.75 |
| | >150 | >150 | 34.59 | 44.78 | 79.37 | 26.41 | 37.34 | 63.75 |
| East | 0-20 | 0-20 | 49.72 | 40.67 | 90.39 | 42.84 | 36.12 | 78.96 |
| | 20-50 | 20-50 | 46.42 | 41.56 | 87.99 | 38.75 | 37.23 | 75.98 |
| | 50-100 | 50-100 | 44.45 | 42.1 | 86.55 | 36.3 | 37.89 | 74.19 |
| | 100-150 | 100-150 | 0 | 0 | 0 | 0 | 0 | 0 |
| | >150 | >150 | 0 | 0 | 0 | 0 | 0 | 0 |
| West | 0-20 | 0-20 | 49.5 | 40.73 | 90.23 | 42.02 | 33.08 | 75.1 |
| | 20-50 | 20-50 | 47.74 | 41.2 | 88.95 | 39.91 | 33.65 | 73.56 |
| | 50-100 | 50-100 | 43.57 | 42.34 | 85.91 | 35.22 | 38.19 | 73.41 |
| | 100-150 | 100-150 | 39 | 43.58 | 82.58 | 30.43 | 39.49 | 69.92 |
| | >150 | >150 | 36.1 | 44.37 | 80.47 | 27.14 | 37.12 | 64.26 |

Analysis of the results shown in *Table 4* also highlights that the reduction in EPgl,nren tends to stabilize for the higher photovoltaic surface area classes. This behaviour indicates a saturation effect: when on-site photovoltaic generation approaches or exceeds the building's energy demand, the additional output does not result in a proportional improvement in the energy index, as the surplus is fed into the grid. From an analytical perspective, this implies that the effectiveness of BIPV in listed historic buildings should not be assessed solely in terms of maximum annual output, but also in relation to the balance between available surface area, the building's energy demand and the actual capacity of renewable generation to offset the non-renewable share.

The same trend is also observed in the analysis extended to the scale of the three districts. In this case, however, the results derive from the extension of the prototype model to the building stock of the districts based on the classification of buildings by roof area and orientation; therefore, the results should be interpreted as an overall assessment of the energy potential of the districts analysed.

Extending the analysis to the district level (*Table 5*) allows verification of the consistency of the results obtained for the prototype building. The three districts analysed show coherent trends, confirming the robustness of the proposed methodological transfer from the building scale to the district scale.

Table 5. $EP_H$ of districts for 2006 and 2050, boiler and boiler + air-to-water heat pump (ASHP)

| Original envelope and boiler system | | | |
|---|---|---|---|
| Districts | Year 2006 $EP_H$ [kWh] | Year 2050 $EP_H$ [kWh] | Reduction [%] |
| 1 | 1866173 | 1688137 | |
| 16 | 1597964 | 1445516 | 9.50 |
| 17 | 1436759 | 1299690 | |
| Improved building envelope and hybrid boiler + air-water heat pump system | | | |
| 1 | 1213842 | 1093219 | |
| 16 | 1039388 | 936100 | 9.94 |
| 17 | 934533 | 841665 | |

At district level, demand for domestic hot water shows a stable and consistent trend in the three areas analysed. No significant differences are observed between the pre- and post-intervention configurations, as DHW demand was evaluated using the same simplified modelling assumptions. Consequently, it is primarily influenced by climatic conditions rather than the configuration of the generation system. The reduction observed in the 2050 scenario compared to 2006 is consistent across all districts and reflects the smaller temperature difference between mains water and supply temperature under future climatic conditions. The overall results are shown in *Table 6*.

Table 6. Annual domestic hot water demand ($EP_W$) of the three districts under pre- and post-intervention configurations, for the 2006 and 2050 climate scenarios.

| Districts | Year 2006 - $EP_w$ [kWh] | | Year 2050 - $EP_w$ [kWh] | |
|---|---|---|---|---|
| | Pre-intervention | Post-intervention | Pre-intervention | Post-intervention |
| 1 | 151430 | 151430 | 58212 | 58212 |

| | | | | |
|---|---|---|---|---|
| 16 | 129667 | 129666 | 49845 | 49845 |
| 17 | 116586 | 116586 | 44817 | 44817 |

Figure 8 shows the trend in on-site renewable energy production generated by BIPV systems as a function of the available roof area and orientation. The results highlight how an increase in the installed PV area leads to a gradual increase in the renewable energy available for heating, with consistently better performance for south-facing roofs. A comparison of the two climate scenarios also shows that, in the future scenario, the production of renewable energy used for heating tends to increase for the same installed area. This behavior is due both to the more favorable operating conditions for heat pumps in the presence of milder outdoor temperatures, and to the expected improvement in the performance of PV modules in future technological scenarios. Conversely, the demand for domestic hot water appears less sensitive to climate variations, reflecting the different relative contributions of the two energy components.

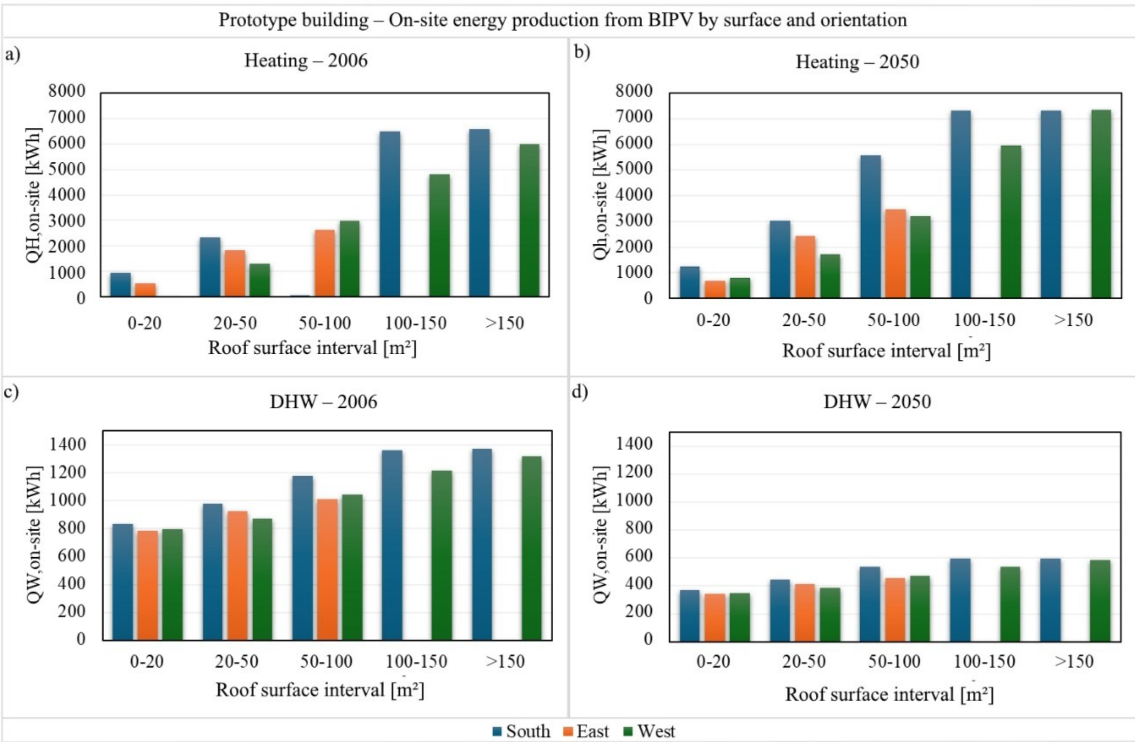


Figure 8. Energy consumption for heating and DHW of the prototype model (Haus Grünhage), by roof orientation and surface, for the climate years 2006 and 2050.

In addition to the aggregate trends observed for the prototype model in Figure 8, the detailed results presented in Appendix A and the trends at district level shown in Figures 9–11 allow for a more explicit interpretation of how roof orientation and available photovoltaic surface area influence the energy balance. South-facing roofs maintain the highest annual performance, as they combine the greatest availability of solar radiation with the greatest reduction in $EP_{gl,nren}$. However, the results also show that west-facing roofs play an increasingly significant role in larger surface area classes, particularly in the 2050 scenario.

This behaviour can be interpreted in light of the temporal distribution of solar generation. Compared to east-facing rooftops, west-facing ones benefit from higher generation during the afternoon hours, which may be more consistent with the operating periods of heat pump-based heating systems. Although this aspect has not been analysed using a specific hourly load matching indicator, Figure 8 and the detailed values reported in Appendix A suggest that the orientation of the roof influences not only the annual photovoltaic yield but also the potential interaction between renewable generation and the building's demand.

Therefore, the optimal BIPV strategy in protected historic centres is not necessarily the maximization of installed PV area, but the identification of the surface-orientation combination that maximizes useful on-site renewable contribution without excessive export.

Figures 9–11 confirm that the trends identified for the prototype are consistently replicated at the district level in Districts 1, 16 and 17, where the gradual increase in available roof area yields cumulative energy benefits, particularly in the 100–150 m² and >150 m² categories. The district-scale graphs should therefore be interpreted as a consistent reproduction, on a larger scale, of the behaviour observed at the prototype level, confirming that the effectiveness of BIPV integration in the historical context analysed depends on the combined effect of roof orientation, available surface area and on-site energy use saturation. The numerical data used to construct the district-scale graphs are presented in Appendix A.

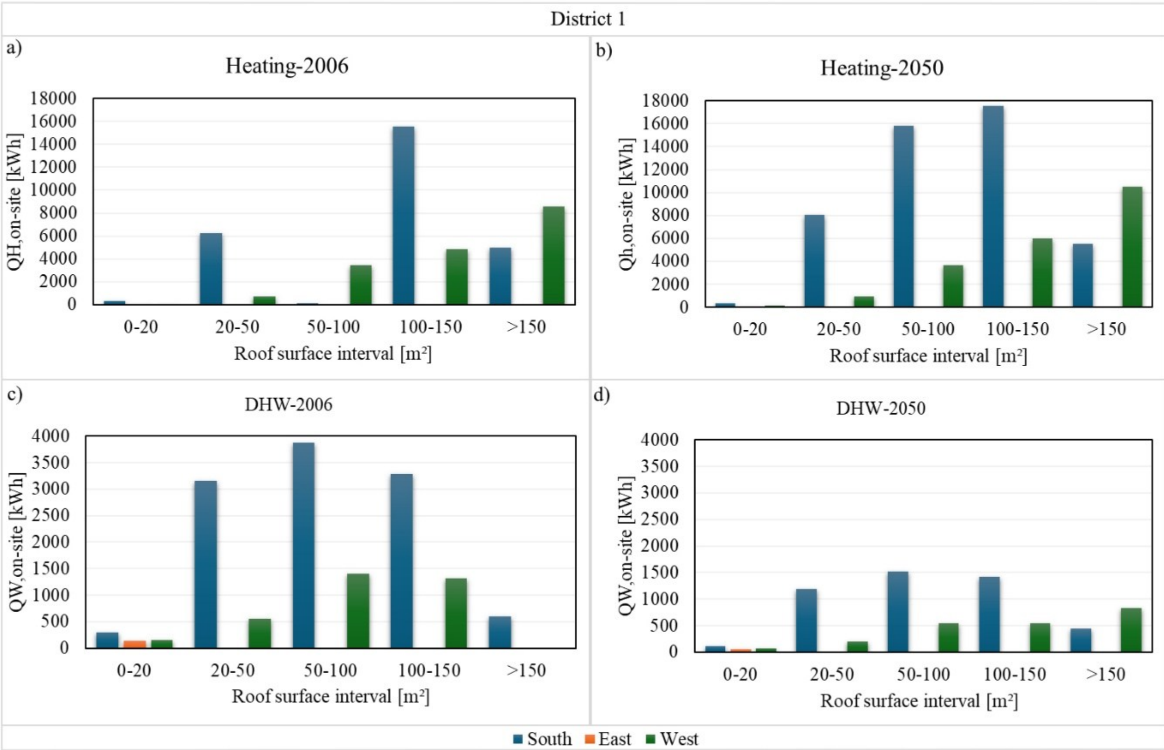


Figure 9. Energy consumption for heating and DHW of District 1, by roof orientation and surface, for the climate years 2006 and 2050.

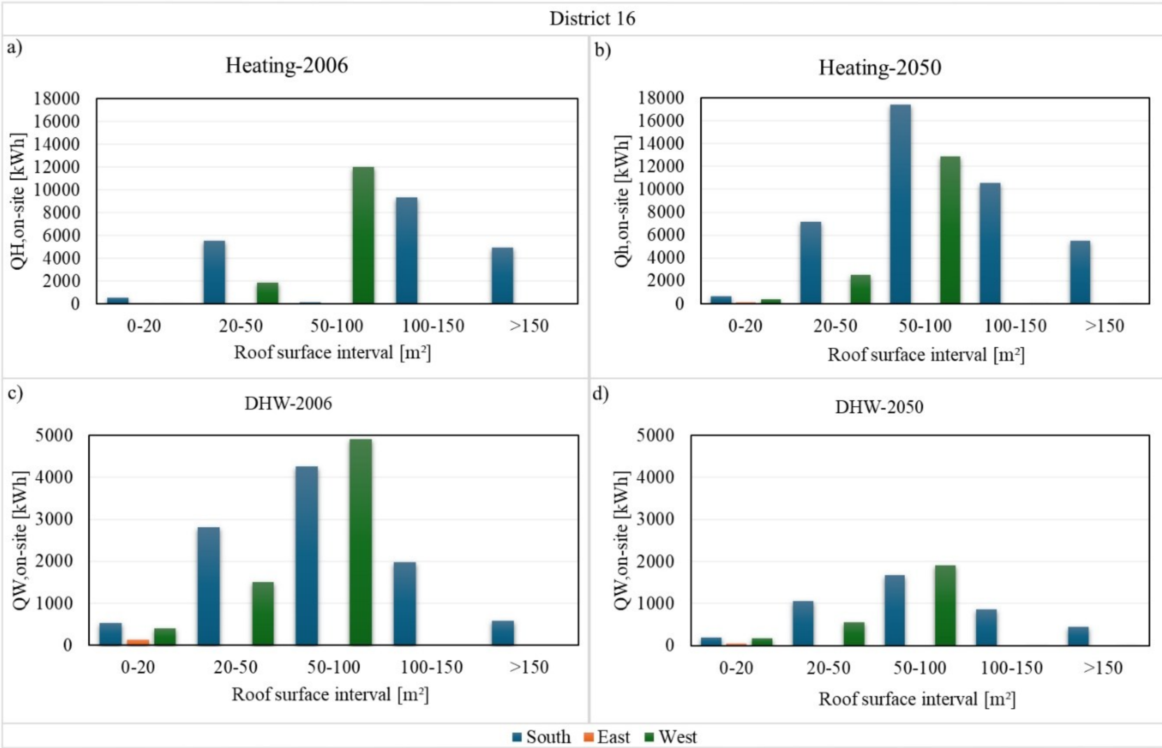


Figure 10. Energy consumption for heating and DHW of District 16, by roof orientation and surface, for the climate years 2006 and 2050.

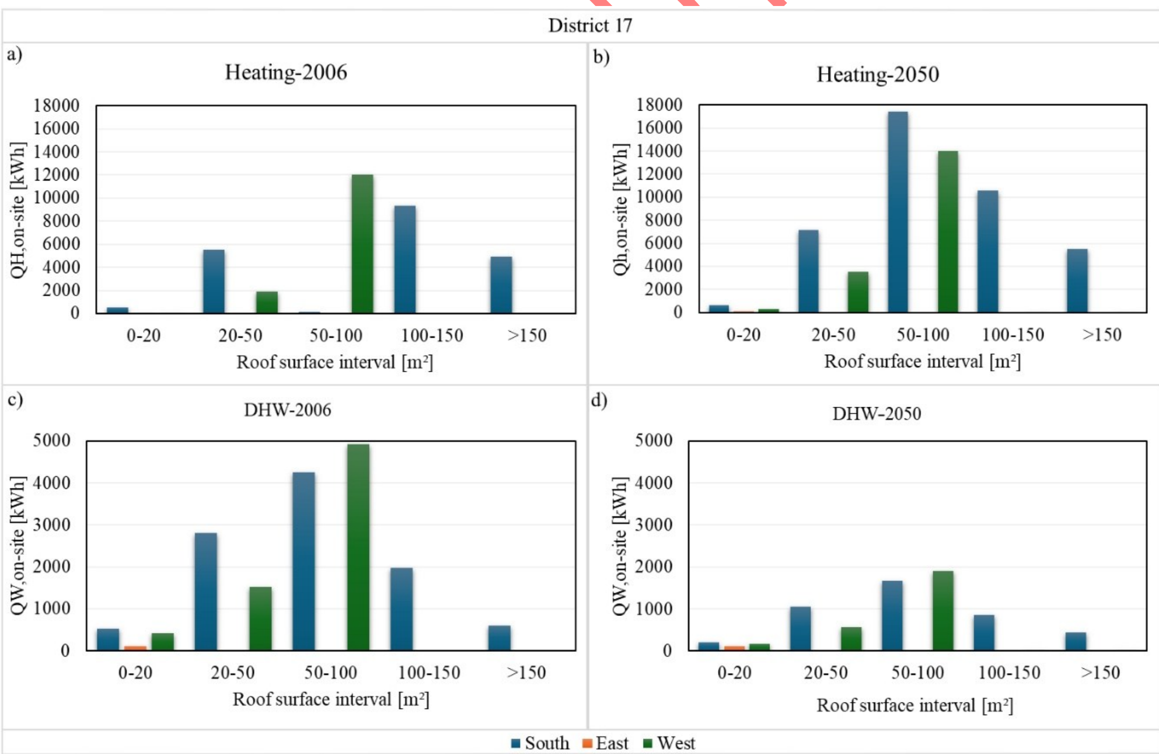


Figure 11. Energy consumption for heating and DHW of District 17, by roof orientation and surface, for the climate years 2006 and 2050.

Overall, a combined analysis of Table 4, Figure 8 and Figures 9–11 shows that the energy savings associated with the retrofit scenario analysed are progressive but not unlimited. Improvements to the building envelope and the integration of the hybrid boiler–heat pump system provide the main reduction in heating demand, whilst BIPV systems further reduce the EPgl,nren depending on the roof orientation and available surface area. The results indicate that the greatest annual benefit is achieved for south-facing roofs and for medium to large available surfaces, whilst further increases in photovoltaic surface area beyond the most effective classes yield diminishing returns due to the saturation of on-site energy use.

The consistency of these trends from the prototype model to Districts 1, 16 and 17 supports the consistency of the comparative extrapolation adopted for the historic fabric analysed. In this sense, BIPV integration should not be interpreted merely as an isolated technological option, but as a complementary measure within a broader decarbonisation strategy, in which improvements to the building envelope, hybrid heating systems and the integration of renewable sources compatible with conservation work together. This integrated approach is particularly relevant in listed historic contexts, where the effectiveness of each intervention depends on technical compatibility, spatial constraints and the balance between on-site demand and renewable generation.

## Conclusions

This study analysed the decarbonization potential of three historic districts in the city of Quedlinburg, which are subject to strict architectural conservation restrictions. The results show that, even in highly protected urban contexts, it is possible to activate effective energy transition pathways through technically compatible and conservation-consistent interventions. The combined application of internal insulation, window replacement and hybrid boiler-heat pump systems has enabled a reduction in heating requirements of over 35% compared to the original configuration. Prospective analysis based on the climate scenario for 2050 shows a further reduction in heating consumption of around 10%, demonstrating how changing climatic conditions can improve the effectiveness of electrified technologies, particularly heat pumps.

At the same time, the use of building-integrated photovoltaic systems, depending on the available surface area and the orientation of the roofs, has led to a significant reduction in the non-renewable primary energy index. On average, the integration of photovoltaic systems enables a reduction of around 30% in the non-renewable primary energy index, with higher values in the most favorable cases. These results confirm that even in contexts subject to stringent landscape constraints, it is possible to achieve significant benefits in terms of energy efficiency and emissions reduction through technological solutions compatible with architectural conservation.

Overall, the methodological approach adopted provides a replicable framework for other European historic centres, demonstrating that targeted interventions consistent with conservation requirements can support progressive decarbonization even where the use of conventional renewable and retrofit solutions is constrained.

Although the results demonstrate the technical feasibility of the proposed strategies, their implementation in protected historic areas depends on local regulatory frameworks, authorization procedures and the involvement of heritage protection authorities. Conservation constraints can influence the applicability of energy technologies, requiring alignment between energy transition objectives and heritage conservation principles. The transferability of the proposed framework therefore depends on the presence of similar typological and regulatory conditions.

The analysis is based on a prototype building considered representative of the prevailing building typology in Quedlinburg's historic centre, which is characterized by marked typological and architectural homogeneity. Accordingly, the results should be interpreted as a comparative district- level assessment rather than as a building-by-building prediction, since variations in maintenance condition, actual use, occupancy patterns, system operation, and previous retrofit interventions may still persist within the building stock, particularly in privately owned dwellings that could not be systematically verified.

## Appendix A

| District | Orientation | Surface interval | No. of buildings | Avg. roof surface | 2006 | | | 2050 | | |
|---|---|---|---|---|---|---|---|---|---|---|
| | | | | | EPgl,nren [kWh/m$^2$] | EPgl,ren [kWh] | EPgl,tot [kWh] | EPgl,nren [kWh/m$^2$] | EPgl,ren [kWh] | EPgl,tot [kWh] |
| 1 | South | **0-20** | 5 | 14.00 | 4088.3936 | 3443.57 | 7531.96 | 3383.03 | 2823.12 | 6206.15 |
| | | **20-50** | 18 | 35.00 | 5472.0411 | 5072.53 | 10544.57 | 4382.48 | 4198.46 | 8580.94 |
| | | **50-100** | 10 | 67.00 | 1405.3731 | 1521.67 | 2927.04 | 1068.43 | 1273.62 | 2342.05 |
| | | **100-150** | 5 | 113.00 | 362.99513 | 465.70 | 828.69 | 275.08 | 388.93 | 664.02 |
| | | **>150** | 1 | 177.00 | 46.002746 | 59.55 | 105.56 | 35.12 | 49.66 | 84.78 |
| | east | **0-20** | 3 | 12.00 | 2926.022 | 2393.43 | 5319.45 | 2521.13 | 2125.66 | 4646.80 |
| | | **20-50** | 0 | 42.00 | 0 | 0 | 0 | 0 | 0 | 0 |
| | | **50-100** | 0 | 59.00 | 0 | 0 | 0 | 0 | 0 | 0 |
| | | **100-150** | 0 | 0.00 | 0 | 0 | 0 | 0 | 0 | 0 |
| | | **>150** | 0 | 0.00 | 0 | 0 | 0 | 0 | 0 | 0 |
| | west | **0-20** | 3 | 14.00 | 2496.9214 | 2054.54 | 4551.46 | 2119.61 | 1668.65 | 3788.26 |
| | | **20-50** | 4 | 31.00 | 1450.064 | 1251.42 | 2701.48 | 1212.23 | 1022.09 | 2234.33 |
| | | **50-100** | 4 | 68.00 | 603.31635 | 586.28 | 1189.60 | 487.69 | 528.82 | 1016.51 |
| | | **100-150** | 2 | 118.00 | 155.60339 | 173.88 | 329.48 | 121.41 | 157.56 | 278.97 |
| | | **>150** | 2 | 168.00 | 101.16595 | 124.34 | 225.51 | 76.06 | 104.02 | 180.08 |
| 16 | South | **0-20** | 9 | 14.00 | 7359.11 | 6198.42 | 13557.53 | 6089.46 | 5081.61 | 11171.08 |
| | | **20-50** | 16 | 35.00 | 4864.04 | 4508.92 | 9372.96 | 3895.53 | 3731.96 | 7627.50 |
| | | **50-100** | 11 | 67.00 | 1545.91 | 1673.83 | 3219.74 | 1175.28 | 1400.98 | 2576.26 |
| | | **100-150** | 3 | 113.00 | 217.80 | 279.42 | 497.21 | 165.05 | 233.36 | 398.41 |
| | | **>150** | 1 | 177.00 | 46.00 | 59.55 | 105.56 | 35.12 | 49.66 | 84.78 |
| | east | **0-20** | 3 | 12.00 | 2926.02 | 2393.43 | 5319.45 | 2521.13 | 2125.66 | 4646.80 |
| | | **20-50** | 0 | 42.00 | 0 | 0 | 0 | 0 | 0 | 0 |
| | | **50-100** | 0 | 59.00 | 0 | 0 | 0 | 0 | 0 | 0 |
| | | **100-150** | 0 | 0.00 | 0 | 0 | 0 | 0 | 0 | 0 |
| | | **>150** | 0 | 0.00 | 0 | 0 | 0 | 0 | 0 | 0 |
| | west | **0-20** | 8 | 14.00 | 6658.46 | 5478.77 | 12137.22 | 5652.29 | 4449.73 | 10102.02 |
| | | **20-50** | 11 | 31.00 | 3987.68 | 3441.40 | 7429.07 | 3333.64 | 2810.75 | 6144.40 |
| | | **50-100** | 14 | 68.00 | 2111.61 | 2052.00 | 4163.60 | 1706.93 | 1850.87 | 3557.79 |
| | | **100-150** | 0 | 118.00 | 0 | 0 | 0 | 0 | 0 | 0 |
| | | **>150** | 0 | 168.00 | 0 | 0 | 0 | 0 | 0 | 0 |
| 17 | sud | **0-20** | 9 | 14.00 | 7359.11 | 6198.42 | 13557.53 | 6089.46 | 5081.61 | 11171.08 |
| | | **20-50** | 16 | 35.00 | 4864.04 | 4508.92 | 9372.96 | 3895.53 | 3731.96 | 7627.50 |
| | | **50-100** | 11 | 67.00 | 1545.91 | 1673.83 | 3219.74 | 1175.28 | 1400.98 | 2576.26 |
| | | **100-150** | 3 | 113.00 | 217.80 | 279.42 | 497.21 | 165.05 | 233.36 | 398.41 |
| | | **>150** | 1 | 177.00 | 46.00 | 59.55 | 105.56 | 35.12 | 49.66 | 84.78 |
| | est | **0-20** | 3 | 12.00 | 2926.02 | 2393.43 | 5319.45 | 2521.13 | 2125.66 | 4646.80 |
| | | **20-50** | 0 | 42.00 | 0 | 0 | 0 | 0 | 0 | 0 |
| | | **50-100** | 0 | 59.00 | 0 | 0 | 0 | 0 | 0 | 0 |
| | | **100-150** | 0 | 0 | 0 | 0 | 0 | 0 | 0 | 0 |
| | | **>150** | 0 | 0 | 0 | 0 | 0 | 0 | 0 | 0 |
| | ovest | **0-20** | 8 | 14.00 | 6658.46 | 5478.77 | 12137.22 | 5652.29 | 4449.73 | 10102.02 |
| | | **20-50** | 11 | 31.00 | 3987.68 | 3441.40 | 7429.07 | 3333.64 | 2810.75 | 6144.40 |
| | | **50-100** | 14 | 68.00 | 2111.61 | 2052.00 | 4163.60 | 1706.93 | 1850.87 | 3557.79 |
| | | **100-150** | 0 | 118.00 | 0 | 0 | 0 | 0 | 0 | 0 |
| | | **>150** | 0 | 168.00 | 0 | 0 | 0 | 0 | 0 | 0 |



## ACKNOWLEDGMENT(S)

This research did not receive any specific funding, and no further acknowledgements are declared.

## NOMENCLATURE

| **Abbreviation** | **Description** |
|---|---|
| ASHP | Air-to-Water Heat Pump |
| BIPV | Building-Integrated Photovoltaics |
| DHW | Domestic Hot Water |
| $EP_{gl}$ | Global Energy Performance Index |

| | |
|---|---|
| $EP_{gl,nren}$ | Non-renewable Global Energy Performance Index |
| $EP_{gl,ren}$ | Renewable Global Energy Performance Index |
| $EP_H$ | Energy Performance Index for Space Heating |
| $EP_W$ | Energy Performance Index for Domestic Hot Water |
| PV | Photovoltaic |
| REC | Renewable Energy Community |
| UNESCO | United Nations Educational, Scientific and Cultural Organization |

## REFERENCES

[1] Sibilio, S., Rosato, A., Ciampi, G., Scorpio, M., Akisawa, A., Building-integrated trigeneration system: Energy, environmental and economic dynamic performance assessment for Italian residential applications, Renewable and Sustainable Energy Reviews, Vol. 68, Part 2, pp. 920–933, 2017, https://doi.org/10.1016/j.rser.2016.02.011.

[2] Matteo, M., Vespasiano, D., Lo Basso, G., Fiorini, C. V., Vallati, A., Performance evaluation of the hybrid heat pump to decarbonize the buildings sector: Energetic, environmental and economic characterization, Energy Engineering, 2025, https://doi.org/10.32604/ee.2025.064353.

[3] Hyldmo, H. da S., Rye, S. A., Vela-Almeida, D., A globally just and inclusive transition? Questioning policy representations of the European Green Deal, Global Environmental Change, Vol. 89, 102946, 2024, https://doi.org/10.1016/j.gloenvcha.2024.102946.

[4] Sousa, J., Lagarto, J., Fonseca, M., The role of storage and flexibility in the energy transition: Substitution effect of resources with application to the Portuguese electricity system, Renewable Energy, Vol. 228, 120694, 2024, https://doi.org/10.1016/j.renene.2024.120694.

[5] Barone, G., Buonomano, A., Forzano, C., Palombo, A., Russo, G., The role of energy communities in electricity grid balancing: A flexible tool for smart grid power distribution optimization, Renewable and Sustainable Energy Reviews, Vol. 187, 113742, 2023, https://doi.org/10.1016/j.rser.2023.113742.

[6] Ahmed, S., Măgurean, A. M., Renewable Energy Communities: Towards a new sustainable model of energy production and sharing, Energy Strategy Reviews, Vol. 55, 101522, 2024, https://doi.org/10.1016/j.esr.2024.101522.

[7] Brunoro, S., Piaia, E., Comunità energetiche per la decarbonizzazione dei borghi storici (in Italian, Energy communities for the decarbonisation of historic villages), in: The 1st International Conference on Net-Zero Built Environment (NTZR 2024), Lecture Notes in Civil Engineering, Vol. 237, Springer, Cham, pp. 1–10, 2025, https://doi.org/10.1007/978-3-031-69626-8_95.

[8] Tsoumanis, G., Formiga, J., Bilo, N., Tsarchopoulos, P., Ioannidis, D., Tzovaras, D., The smart evolution of historical cities: Integrated innovative solutions supporting the energy transition while respecting cultural heritage, Sustainability, Vol. 13, 9358, 2021, https://doi.org/10.3390/su13169358.

[9] Rosa, F., Building-integrated photovoltaics (BIPV) in historical buildings: Opportunities and constraints, Energies, Vol. 13, 3628, 2020, https://doi.org/10.3390/en13143628.

[10] P. A. Lombardi, M. Richter, P. Komarnicki, Balancing preservation and progress: A digital Platform for Decarbonizing Heritage City Centers", IEEE International Humanitarian Technologies Conference (IHTC), Bari 30.11.2025

[11] A. Semenyuk, A. Höpfner, P. A. Lombardi, M. Richter, S. Stüring, P. Komarnicki, „Interdisciplinary urban planning in VR: Virtual twins for sustainable urban development!, IEEE International Smart Cities Conference (SSC2), 24.09.2023

[12] Cabeza, L. F., de Gracia, A., Pisello, A. L., Integration of renewable technologies in historical and heritage buildings: A review, *Energy and Buildings*, Vol. 177, pp. 96–111, 2018, https://doi.org/10.1016/j.enbuild.2018.07.058.

[13] Hilber, C. A. L., Palmer, C., Pinchbeck, E. W., The energy costs of historic preservation, Journal of Urban Economics, Vol. 114, 103197, 2019, https://doi.org/10.1016/j.jue.2019.103197.

[14] Caputo, P., Ferrari, S., Ferla, G., Zagarella, F., Preliminary energy assessments for the energy retrofit of protected rural buildings in a peripheral context of Milan, Journal of Sustainable Development of Energy, Water and Environment Systems, Vol. 8, No. 4, pp. 715–734, 2020, https://doi.org/10.13044/j.sdewes.d8.0332.

[15] Blumberga, A., Freimanis, R., Muizniece, I., Spalvins, K., Blumberga, D., Trilemma of historic buildings: Smart district heating systems, bioeconomy and energy efficiency, Energy, Vol. 186, 115741, 2019, https://doi.org/10.1016/j.energy.2019.07.071.

[16] Nair, G., Verde, L., Olofsson, T., A review on technical challenges and possibilities on energy efficient retrofit measures in heritage buildings, Energies, Vol. 15, 7472, 2022, https://doi.org/10.3390/en15207472.

[17] Moghaddam, S. A., Mattsson, M., Ameen, A., Akander, J., da Silva, M. G., Simões, N., Low-emissivity window films as an energy retrofit option for a historical stone building in cold climate, Energies, Vol. 14, 7584, 2021, https://doi.org/10.3390/en14227584.

[18] Korkmaz, E., Kurkcuoglu, M. A. S., Analysis of the socio-spatial vulnerabilities to energy poverty factors of Türkiye, Energy and Buildings, Vol. 330, 115343, 2025, https://doi.org/10.1016/j.enbuild.2025.115343.

[19] Di Rocco, A. R., Bottino-Leone, D., Troi, A., Herrera-Avellanosa, D., Application of the guidelines for the integration of photovoltaics in historic buildings and landscapes to evaluate the best practices of the Historic Building Energy Retrofit Atlas, Buildings, Vol. 14, 499, 2024, https://doi.org/10.3390/buildings14020499.

[20] Pérez-Pérez, B., Chacón-Linares, E., Transition and heritage in the Anthropocene era—proposal for a methodological analysis at local scale, Urban Science, Vol. 9, 112, 2025, https://doi.org/10.3390/urbansci9040112.

[21] Lucchi, E., Integration between photovoltaic systems and cultural heritage: A socio-technical comparison of international policies, design criteria, applications, and innovation developments, Energy Policy, Vol. 171, 113303, 2022, https://doi.org/10.1016/j.enpol.2022.113303.

[22] Congedo, P. M., Palmieri, A., Baglivo, C., Climate resilience strategies for schools in Mediterranean areas: Is it feasible to condition air merely with ventilation?, Energy Efficiency, Vol. 18, Art. 24, 2025, https://doi.org/10.1007/s12053-025-10311-7.

[23] Congedo, P. M., Palmieri, A., Baglivo, C., Optimizing ventilation strategies for thermal comfort in Mediterranean schools: A dynamic modeling approach, Energies, Vol. 18, Art. 1542, 2025, https://doi.org/10.3390/en18061542.

[24] De Medici, S., Italian architectural heritage and photovoltaic systems: Matching style with sustainability, Sustainability, Vol. 13, 2108, 2021, https://doi.org/10.3390/su13042108.

[25] Polo López, C. S., Troia, F., Nocera, F., Photovoltaic BIPV systems and architectural heritage: New balance between conservation and transformation, Sustainability, Vol. 13, 5107, 2021, https://doi.org/10.3390/su13095107.

[26] Sigounis, A.-M., Vallianos, C., Athienitis, A., Model predictive control of air-based building integrated PV/T systems for optimal HVAC integration, Renewable Energy, Vol. 212, pp. 655–668, 2023, https://doi.org/10.1016/j.renene.2023.05.059.

[27] Marchini, F., Chiatti, C., Fabiani, C., Pisello, A. L., Development of an innovative translucent–photoluminescent coating for smart windows applications: An experimental and numerical investigation, Renewable and Sustainable Energy Reviews, Vol. 184, 113530, 2023, https://doi.org/10.1016/j.rser.2023.113530.

[28] Bogdanov, D., Satymov, R., Breyer, C., Impact of temperature dependent coefficient of performance of heat pumps on heating systems in national and regional energy systems modelling, Applied Energy, Vol. 371, 123647, 2024, https://doi.org/10.1016/j.apenergy.2024.123647.

[29] Land Sachsen-Anhalt, Denkmalschutzgesetz des Landes Sachsen-Anhalt (DSchG LSA), GVBl. LSA 1991, p. 368, amended by Art. 2 of the law of 20 December 2005 (GVBl. LSA p. 769), available online, https://www.kulturstiftungst.de/fileadmin/user_upload/06_Metaseiten/Footer/Denkmalschutzgesetz_des_Landes_Sachsen_Anhalt.pdf, accessed 30 June 2025.

[30] DIN Deutsches Institut für Normung (DIN), Thermal protection and energy economy in buildings – Part 2: Minimum requirements for thermal insulation, DIN 4108-2:2013-02, Berlin, Germany, 2013, available online, accessed on 30 June 2025.

[31] Arnfield, A. J., Köppen climate classification, Encyclopaedia Britannica, 16 October 2023, https://www.britannica.com/science/Koppen-climate-classification, accessed 30 June 2025.

[32] Renewables.ninja, Renewables.ninja platform, available online, https://www.renewables.ninja/, accessed 9 March 2025.

[33] Meteonorm. Global Meteorological Database; Meteotest: Bern, Switzerland, 2012; Available online: https://meteonorm.com/en/ (accessed on 16 July 2025)

[34] Congedo, P. M., Baglivo, C., Seyhan, A. K., Marchetti, R., Worldwide dynamic predictive analysis of building performance under long-term climate change conditions, Journal of Building Engineering, Vol. 42, 103057, 2021, https://doi.org/10.1016/j.jobe.2021.103057.

[35] Paolo Maria Congedo, Cristina Baglivo, Delia D'Agostino, Domenico Mazzeo,The impact of climate change on air source heat pumps, Energy Conversion and Management, Volume 276, 2023, 116554, ISSN 0196-8904, https://doi.org/10.1016/j.enconman.2022.116554.

[36] Chengjian Xu, Olindo Isabella, Malte Ruben Vogt, Future material demand for global silicon-based PV modules under net-zero emissions target until 2050, Resources, Conservation and Recycling, Volume 210, 2024, 107824, ISSN 0921-3449, https://doi.org/10.1016/j.resconrec.2024.107824.

[37] Quedlinburg 3D Viewer, Dronodat DVQDB-Beta, available online, https://dronodat.com/dvqdb-beta/, accessed 16 September 2025.